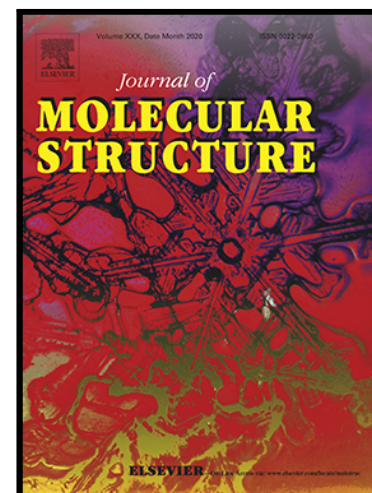


Journal Pre-proof

Energetic features of antiparallel stacking and hydrogen bonding interactions in two coordination complexes bearing 1,10-phenanthroline-2,9-dicarboxylic acid



Mahmood Akbari , Masoud Mirzaei , Amir Sh Saljooghi ,
Samaneh Sadeghzadeh , Nahid Lotfian , Maral Aghamohammadi ,
Behrouz Notash , Joel T. Mague , Rosa M. Gomila ,
Antonio Frontera

PII: S0022-2860(21)02084-6
DOI: <https://doi.org/10.1016/j.molstruc.2021.131963>
Reference: MOLSTR 131963

To appear in: *Journal of Molecular Structure*

Received date: 20 September 2021
Revised date: 7 November 2021
Accepted date: 17 November 2021

Please cite this article as: Mahmood Akbari , Masoud Mirzaei , Amir Sh Saljooghi , Samaneh Sadeghzadeh , Nahid Lotfian , Maral Aghamohammadi , Behrouz Notash , Joel T. Mague , Rosa M. Gomila , Antonio Frontera , Energetic features of antiparallel stacking and hydrogen bonding interactions in two coordination complexes bearing 1,10-phenanthroline-2,9-dicarboxylic acid, *Journal of Molecular Structure* (2021), doi: <https://doi.org/10.1016/j.molstruc.2021.131963>

This is a PDF file of an article that has undergone enhancements after acceptance, such as the addition of a cover page and metadata, and formatting for readability, but it is not yet the definitive version of record. This version will undergo additional copyediting, typesetting and review before it is published in its final form, but we are providing this version to give early visibility of the article. Please note that, during the production process, errors may be discovered which could affect the content, and all legal disclaimers that apply to the journal pertain.

© 2021 Published by Elsevier B.V.

Highlights

- Two new cobalt and cerium complexes with π -extended organic ligands have been synthesized and characterized.
- Cerium complex with 1,10-phenanthroline-2,9-dicarboxylate (PDA) and water form of left-handed and right-handed helices.
- Cobalt complex with PDA and 1,10-phenanthroline (phen) has a strong tendency to form antiparallel π -stacking assemblies.
- Supramolecular assemblies studied by means of DFT calculations

Journal Pre-proof

Energetic features of antiparallel stacking and hydrogen bonding interactions in two coordination complexes bearing 1,10-phenanthroline-2,9-dicarboxylic acid

Mahmood Akbari,^a Masoud Mirzaei,^{*a} Amir Sh. Saljooghi,^a Samaneh Sadeghzadeh,^a Nahid Lotfian,^a Maral Aghamohammadi,^a Behrouz Notash,^b Joel T. Mague,^c Rosa M. Gomila,^d and Antonio Frontera^{*d}

^aDepartment of Chemistry, Faculty of Science, Ferdowsi University of Mashhad, PO Box 9177948974, Mashhad, Iran, E-mail: mirzaeesh@um.ac.ir

^bDepartment of Inorganic Chemistry and Catalysis, Shahid Beheshti University, Tehran, Iran

^cDepartment of Chemistry, Tulane University, New Orleans, LA, 70118, USA

^dDepartament de Química, Universitat de les Illes Balears, Crta de Valldemossa km 7.5, 07122 Palma de Mallorca (Balears), SPAIN, E-mail: toni.frontera@uib.es

Highlights:

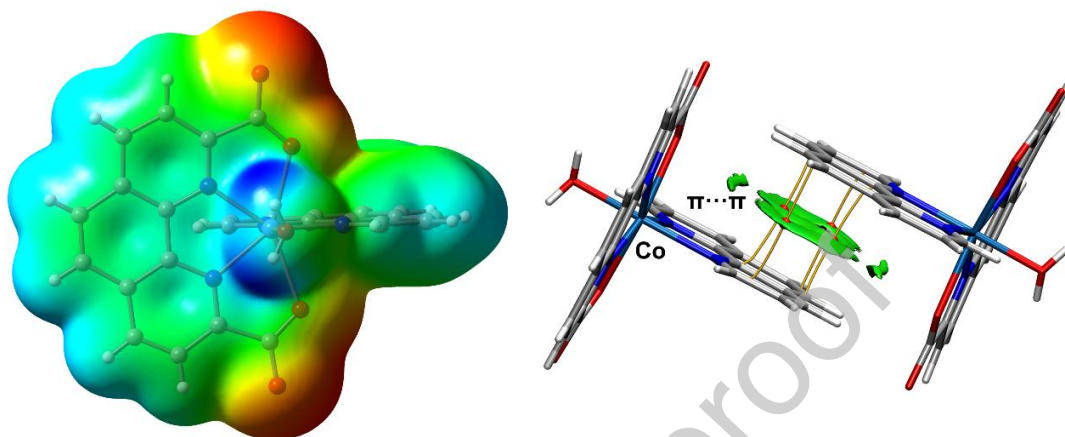
- Two new cobalt and cerium complexes with π -extended organic ligands have been synthesized and characterized.
- Cerium complex with 1,10-phenanthroline-2,9-dicarboxylate (PDA) and water form of left-handed and right-handed helices.
- Cobalt complex with PDA and 1,10-phenanthroline (phen) has a strong tendency to form antiparallel π -stacking assemblies.
- Supramolecular assemblies studied by means of DFT calculations

Graphical Abstract (text)

This manuscript reports the synthesis, X-ray characterization and DFT studies of two new metal–organic complexes, $[\text{Co}(\text{phen})(\text{PDA})\text{H}_2\text{O}] \cdot \text{CH}_3\text{CN} \cdot \text{H}_2\text{O}$ (**1**), (*phen* = 1,10-phenanthroline, PDA = 1,10-phenanthroline-2,9-dicarboxylate) and $[\text{Ce}_2(\text{PDA})_3(\text{H}_2\text{O})_2] \cdot 3\text{H}_2\text{O}$ (**2**). The energetic

features of the antiparallel stacking and H-bonding interactions are reported and discussed in detail.

Graphical Abstract



ABSTRACT

Two new metal–organic complexes, $[\text{Co}(\text{phen})(\text{PDA})\text{H}_2\text{O}] \cdot \text{CH}_3\text{CN} \cdot \text{H}_2\text{O}$ (**1**), (*phen* = 1,10-phenanthroline, PDA = 1,10-phenanthroline-2,9-dicarboxylate) and $[\text{Ce}_2(\text{PDA})_3(\text{H}_2\text{O})_2] \cdot 3\text{H}_2\text{O}$ (**2**) have been synthesized and characterized by elemental analysis, infrared spectroscopy, and single-crystal X-ray crystallography. Structural characterization by single-crystal X-ray diffraction shows that in **1** the cobalt ion forms a discrete seven-coordinated complex with a distorted pentagonal bipyramidal geometry around the metal centre. These discrete units are further packed into 3-D supramolecular assemblies by different kinds of the noncovalent interactions. Complex **2** consists of a 1D coordination polymeric structure with the cerium ion coordinated by PDA and water in the form of left-handed and right-handed helices. The extended aromatic systems of PDA and *phen* have a strong tendency to establish antiparallel $\pi \cdots \pi$ stacking interactions generating interesting assemblies in the solid state of **1**. They have been studied theoretically using DFT calculations and characterized by means of the quantum theory of “atoms-in-molecules” (QTAIM) and the noncovalent interaction (NCI) plot methods. This study is useful to understand in more detail the energetic and structural stability of these categories of metal-organic complexes. The results reported herein suggest that the antiparallel π -stacking interactions involving the neutral and, in principle innocent, *phen* auxiliary ligand are energetically very relevant in the solid state of **1**.

Keywords: Antiparallel $\pi \cdots \pi$ stacking interaction, Cerium, Cobalt, Single-crystal X-ray crystallography, Noncovalent interaction.

1. Introduction

The design and construction of new metal-organic coordination compounds are of current interest in the fields of crystal engineering [1-3]. Supramolecular engineering is gaining interest, since it provides a rational strategy for designing various crystalline materials, which can be constructed from basic building blocks with appropriate structure-directing groups for intermolecular contacts, such as coordination bonds and weak intermolecular interactions. Generally, the metal-ligand ratio, conformation, connectivity, dimensionality, and packing in the final product depend on the components of the network and experimental conditions [4]. In this regard, the selection of appropriate organic ligands as structure-directing agents is crucial [5]. Among various organic ligands, aromatic N-heterocyclic multi-carboxylic acids are valuable in this context because they can act as good bridging ligands between two transition metal or lanthanide ions and the rigidity of the aromatic part favors the formation of ordered single crystals [6-8]. From the point of view of ligand design, 1,10-phenanthroline-2,9-dicarboxylic acid (H_2PDA), with its large conjugated aromatic plane, rigid phenanthroline skeleton, two donor nitrogen atoms and two negatively charged carboxylate groups, is one of the most prominent such ligands [9]. The structural properties of this ligand increase its ability to coordinate to metal ions. It was observed that the coordination mode of PDA is highly dependent on the size of the metal ion. Hancock reported the formation constants for complexing of series of metal ions with PDA in aqueous media and showed that PDA displays a strong size selectivity, due to the formation of three rigid, five-membered chelate rings in final product [10-13]. For instance, small transition metal ions such as $Co(II)$, are coordinated in a tridentate fashion [14], while lanthanoid ions with higher ionic radii can bind to all four donor atoms of the PDA ligand [15]. In previous work, we reported on the design and synthesis of various coordination compounds derived from H_2PDA as a ligand [16-21]. As an extension of our previous work, we report here on the hydrothermal synthesis of a $Co(II)$ and a $Ce(III)$ complex of the PDA ligand with the former also containing 1,10-phenanthroline (*phen*) as an ancillary ligand. These two new complexes have different dimensionalities and are formulated as $[Co(phen)(PDA)H_2O] \cdot CH_3CN \cdot H_2O$ (**1**) and $[Ce_2(PDA)_3(H_2O)_2]_n \cdot 3nH_2O$ (**2**). The selection of

Co(II) and Ce(III) metal center was motivated by their large difference in atomic radius (~30 pm) since we were interested in analyzing their different behavior towards the primary and auxiliary ligands (*phen* and PDA, respectively). Moreover, theoretical investigations (DFT-D3 calculations) have been performed with the purpose to (i) study the noncovalent interactions observed in the 3D supramolecular assemblies of compound **1** and (2) characterize them using the Bader's quantum theory of "atoms-in-molecules" [22] combined with the noncovalent interaction plot (NCIPlot) index method [23]. The latter is very convenient to reveal noncovalent interactions in real space. The combination of theory and experiment reported herein provides valuable information for researchers working in crystal engineering, supramolecular and coordination chemistry, since coordination complexes containing 1,10-phenanthroline-2,9-dicarboxylic acid are scarce in the literature. The strong influence of metal coordination on the strength of the π -stacking interactions have been confirmed using DFT calculations and NCI plot computational tools. Indeed, the strength of the π - π stacking interaction is enhanced by the coordination to the cobalt centres, due to the amplification of the dipole-dipole force. They have been designed to investigate the effect of primary and secondary ligands on the crystalline lattice and non-covalent interactions in this type of coordination complexes.

2. Experimental

2.1. Materials and general methods

All reagents were commercially purchased and used without further purification except for PDA which was synthesized according to a reported procedure [24]. IR spectra of sample in a KBr disc were recorded on a Buck 500 spectrometer. Elemental analyses (CHN) were performed using a Thermo Finnigan Flash EA 1112 microanalyzer.

2.2. Syntheses

Synthesis of 1: A mixture of $\text{Co}(\text{CH}_3\text{COO})_2 \cdot 4\text{H}_2\text{O}$ (0.050 g, 0.2 mmol), H_2PDA (0.050 g, 0.2 mmol), *phen* (0.072 g, 0.4 mmol) and MeOH/MeCN (10 mL, v/v = 1/1) was stirred for about two hours in air. The mixture was then transferred to a 23 mL Teflon-lined autoclave and kept at 160 °C for 3 days. After slow cooling (2 °C h⁻¹) to room temperature, the product was isolated as light brown crystals in 80% yield based on Co. Anal. Calcd. for $\text{C}_{28}\text{H}_{21}\text{CoN}_5\text{O}_6$: C 57.74, H 3.63,

N 12.02 %; Found C 57.19, H 3.40, N 11.94 %. IR (KBr pellet, cm^{-1}) ν : 3419 (bs), 3223 (bs), 1615 (s), 1567 (s), 1508 (w), 1425 (w), 1370 (s), 1316 (m), 1196 (w), 1140 (w), 879 (m), 850 (m), 802 (m), 720 (m).

Synthesis of 2: A mixture of $\text{Ce}(\text{NO}_3)_3 \cdot 6\text{H}_2\text{O}$ (0.108 mg, 0.25 mmol), H_2PDA (0.067 g, 0.25 mmol) and H_2O was stirred for about an hour in air and the pH was adjusted to about 4.5 with NaOH solution. The mixture was then transferred to a 23 mL Teflon-lined autoclave and kept at 130 °C for 2 days. After slow cooling (2°C h^{-1}) to room temperature, the reaction mixture was filtered and the filtrate was kept at room temperature for slow evaporation. Yellow crystals of **2** were obtained over the course of 10 days in 60% yield based on Ce. Anal. Calcd. for $\text{C}_{42}\text{H}_{28}\text{Ce}_2\text{N}_6\text{O}_{17}$: C 43.15, H 2.41, N 7.19 %; Found C 43.01, H 2.60, N 7.02 %. IR (KBr pellet, cm^{-1}) ν : 3740 (bs), 3462 (bs), 1639 (s), 1560 (s), 1455 (m), 1377 (s), 1305 (m), 1184 (w), 880 (m), 806 (s), 712 (m).

2.3. X-ray Crystallography

For **1**, the X-ray diffraction measurements were carried out on a STOE IPDS 2T diffractometer with graphite-monochromated $\text{MoK}\alpha$ radiation. The single crystal was mounted on a glass fiber and used for data collection. Cell constants and orientation matrixes for data collection were obtained by least-square refinement of the setting angles for 1328 reflections. Diffraction data were collected in a series of ω scans in 1° oscillations and integrated using the Stoe X-AREA software package [25]. Numerical absorption corrections were applied using the WinGX-2013.3 software [26]. The structure was solved by direct methods and subsequent difference Fourier maps and then refined on F^2 by a full-matrix least-squares procedure using anisotropic displacement parameters. Atomic factors are from the International Tables for X-ray Crystallography [27]. All non-hydrogen atoms were refined with anisotropic displacement parameters. Hydrogen atoms were placed in ideal positions and included as riding atoms with relative isotropic displacement parameters. All refinements were performed using the X-STEP32 [28] and SHELXL [29] programs.

For **2**, the X-ray intensity data were measured on a Bruker Smart APEX CCD diffractometer equipped with a fine-focus sealed tube ($\text{Mo-K}\alpha$, $\lambda = 0.71073 \text{ \AA}$) and a graphite

monochromator. A suitable crystal was chosen using a polarizing microscope, covered with a film of heavy oil and mounted on a polymer loop for data collection. Crystallographic data were collected at a temperature of 150(2) K to a maximum 2θ value of 33.199° and integrated with Bruker SAINT [30] using a narrow-frame algorithm. Data were corrected for absorption effects using the multi-scan method (SADABS) [30-31]. The structure was solved using SHELXT [32] and refined with SHELXL [33] with the hydrogen atoms included as riding contributions in idealized positions with isotropic displacement parameters tied to those of the attached atoms. A summary of refinement parameters is given in Table 1.

2.4 Theoretical Methods

The interaction energies were computed at the RI-BP86-D3/def2-TZVP [34-37] level of theory with the Turbomole 7.0 program [38] and the crystallographic coordinates as starting points. The counterpoise method was used to avoid the basis set superposition error [39]. For the Co(II) d^7 metal centre the high spin configuration (three unpaired electrons) was used since it is energetically more stable than the low spin (one unpaired electron). The 0.001 a.u. isosurface was used for molecular electrostatic potential (MEP) surface calculations. The QTAIM [22] and NCIPLOT [40] analyses have been performed using the Multiwfn program [41] and represented using the VMD visualization software [42].

3. Results and Discussion

3.1. Synthesis

Complexes **1** and **2** have been synthesized from H₂PDA under hydrothermal conditions. The conditions reported in the Experimental Section have been optimized for yields of pure crystalline products. When we used Co(II) ion and *phen* as an auxiliary ligand, the resulting complex (**1**) had a discrete monomer structure. Replacing Co(II) with Ce(III) and eliminating the *phen* auxiliary ligand led to the formation of a 1-D coordination polymer (**2**).

3.2 Crystal structures

3.2.1. Structure description of 1

As shown in Figure 1, **1** is a mononuclear complex and the asymmetric unit consists of one Co(II) ion, one PDA ligand, one *phen* ligand, one coordinated water molecule, one uncoordinated water molecule and one uncoordinated acetonitrile molecule. The coordination geometry around the Co(II) centre and the coordination modes of the PDA and *phen* ligands in **1** are shown in Figure S1 (ESI). The Co(II) ion is seven-coordinate (CoN_4O_3) and exhibits a distorted pentagonal bipyramidal (PBP) geometry, being bound by two carboxylate O atoms from the PDA ligand [$\text{Co-OPDA} = 2.391(3)$ and $2.409(3)$ Å], two N atoms of the PDA ligand [$\text{Co-NPDA} = 2.146(4)$ and $2.158(4)$ Å], two N atoms of the phenanthroline ligand [$\text{Co-Nphen} = 2.102(5)$ and $2.183(5)$ Å] and the O atom of a water molecule [$\text{Co-O(water)} = 2.130(3)$ Å]. In **1**, the PDA is thus bound as a tetradentate chelate ligand.

In **1**, the O–H \cdots O (along the $(-19\ 19\ 1)$ plane) and C–H \cdots O (along $(0\ 0\ 1)$ plane) hydrogen bonds form several graph sets (Figures S2 and S3). The strong O–H \cdots O hydrogen bonds between the coordinated/uncoordinated water molecules and the uncoordinated carboxylate oxygen atoms of PDA form a $R_2^2(12)$ graph set (Figure 2) and three different chain motifs ($C_4^4(22)$, $C_2^2(12)$ and $C_2^2(10)$) generating an infinite, zigzag chain along the $(-19\ 19\ 1)$ direction (Figure S3).

As shown in Figure 3, this compound also forms two different self-assembled dimers guided by $\pi\cdots\pi$ stacking interactions in the solid state. One involves the PDA rings from two neighboring units with a centroid \cdots centroid separation of 3.454 Å (Figure 3a) and the other one the *phen* ligands with a longer centroid \cdots centroid separation of 3.808 Å (Figure 3b). Both interactions are further analyzed below (theoretical section) where the dimerization energies are compared.

3.2.1. Structure description of 2

The asymmetric unit of **2** is composed of two crystallographically unique Ce(III) ions, three PDA ligands, two coordinated water molecules, and three uncoordinated water molecules (Figure 4). The Ce1 centre is eight-coordinate and appears most closely described as having a dodecahedral geometry with coordination by four carboxylate oxygen atoms [$\text{Ce1-O}_{\text{carboxylate}} = 2.410(1)$ – $2.475(1)$ Å] and four nitrogen atoms of the phenanthroline rings [$\text{Ce-N} = 2.624(1)$ –

2.645(1) Å] from two PDA ligands. The Ce2 centre is coordinated to four carboxylate oxygen atoms from three PDA ligands [Ce2–O_{carboxylate} = 2.416(1)–2.473(1) Å], two nitrogen atoms of the phenanthroline rings of one organic ligand [Ce2–N = 2.654(1) and 2.656(1) Å] and two water molecules [Ce2–O = 2.482(1) and 2.503(1) Å]. The Ce ions and PDA ligands build helical chains extending parallel to the b axis (Figure 5a). The whole structure of **2** is racemic due to the presence of right-handed and left-handed helices packing in an ABAB fashion (Figure 5b).

3.3 Theoretical study

This study is mainly focused on **1** since **2** is polymeric and, consequently, its solid state architecture is dominated by coordination bonds. In particular, we have studied in **1** the formation of the supramolecular assemblies directed by the H-bonding (the $R_2^2(12)$ assembly shown in Figure 2) and the antiparallel $\pi \cdots \pi$ interactions (self-assembled dimers shown in Figure 3). The molecular electrostatic potential (MEP) surface plot of **1** was used to recognize the most electron rich and electron poor parts of the compound (Figure 6). The MEP maxima are located at the protons of the coordinated water molecule (+43.9 kcal/mol). The most negative MEP value is located at the O-atoms of the 1,10-phenanthroline-2,9-dicarboxylate groups (–59.9 kcal/mol), as expected. The MEP values are also positive above and below the PDA ligand (ranging from +8.8 to +11.9 kcal/mol) and at the aromatic H-atoms of the ligand (+27.6 kcal/mol). The MEP values over the aromatic rings of the *phen* ligand are smaller than those observed for the PDA ligand, ranging from –3.1 to +4.4 kcal/mol.

Fig. 7 shows the combined QTAIM/NCIplot analysis of the $R_2^2(12)$ dimer of **1** confirming the existence of two symmetrically equivalent H-bonds, each one characterized by a bond critical point (represented by a small red sphere) and bond path connecting the H-atom of the coordinated water molecule to the O-atom of the carboxylate group. The existence and strong nature of this H-bond is confirmed by the NCIplot index analysis that reveals a small and blue isosurface coincident to the location of the bond CP. The NCIplot analysis also reveals the existence of an extended green isosurface between both monomers, basically located between the uncoordinated O-atoms of the carboxylate groups and one five-membered chelate ring (CR), thus suggesting the existence of two symmetrically equivalent O \cdots CR interactions and π -stacking of

the carboxylate groups, since a bond CP and bond path interconnect the C-atoms of these groups. This combination of factors explains the large dimerization energy ($\Delta E_1 = -27.3$ kcal/mol) and confirms the crucial role of the $R_2^2(12)$ synthon in the solid state architecture of **1**. Moreover, we have estimated the strength of each H-bond by using the value of the potential energy density at the bond CPs. To do so, we have used the equation proposed by Espinosa *et al.* ($E = 0.5 \cdot V_r$) [43] and the energy values are shown adjacent to the bond CPs, showing that the contribution of each H-bond is -5.30 kcal/mol, so the total contribution due to the H-bonds is -10.6 kcal/mol. This result suggests that the $O \cdots CR/\pi \cdots \pi$ interaction is stronger than the sum of the H-bonds and dominant in the formation of the dimer.

We have further analyzed the $\pi \cdots \pi$ self-assembled dimers described in Figure 3. The combined QTAIM/NCIplot index analysis of the dimer where the PDA units are stacked is shown in Fig. 8a. Remarkably, six bond CPs, and bond paths interconnect the six C-atoms of the central rings of the PDA moieties, thus evidencing a large overlap of the π -systems. The interaction is characterized by two additional bond CPs that interconnect two C-atoms of the fused pyridine rings. Moreover, a green NCIplot isosurface, basically located between the phenyl rings of the PDA ligand, is also observed, in agreement with the QTAIM analysis. The interaction energy is moderately strong ($\Delta E_2 = -13.1$ kcal/mol), confirming the importance of the antiparallel π -stacking interaction. Figure 8b shows the QTAIM/NCIplot analysis of the antiparallel π -stacking dimer involving the *phen* ligand. In this case four bond CPs and bond path interconnect four C-atoms of organic ligand. The QTAIM analysis shows an extended green isosurface that embraces two six-membered rings of the ligands. In this case, the dimerization energy is very large ($\Delta E_3 = -26.2$ kcal/mol) and shows that this π -stacking mode involving *phen* ligands is more important than the π -stacking mode involving PDA ligands. This is likely due to larger electrostatic repulsion in the PDA \cdots PDA stacking (this is obviously compensated by the dominant dispersion and polarization forces of this type of interaction). This electrostatic repulsion is smaller in the *phen* \cdots *phen* stacking because the MEP values over the aromatic rings involved in the interaction are smaller. The *phen* \cdots *phen* stacking dimer exhibits a dimerization energy that is similar to the $R_2^2(12)$ dimer thus confirming its importance in the solid state of **1**.

4. Concluding remarks

The manuscript presents a combined experimental and theoretical investigation about the metal complexation and crystal form of some metal-organic complexes based on the 1,10-phenanthroline-2,9-dicarboxylic acid ligand. The research topic explored in the manuscript is of interest since it helps us to understand in more detail the energetic and structural stability of these metal-organic complexes. From scientific point of view, the present manuscript provides a valuable methodological discussion and analysis about the ability of the Co(II) and Ce(III) metals to create high-order ligand coordination and form metal-organic crystals. The influence of the metal coordination on the strength of the π -stacking interactions has been considered using DFT calculations and NCI plot index analysis. When Co(II) is selected as a transition metal ion and *phen* as an auxiliary ligand, the resulting compound has a discrete, monomeric structure. However, by using Ce(III) as a lanthanoid ion with higher ionic radii and eliminating the *phen* as an auxiliary ligand an 1-D coordination polymeric structure is formed (**2**). The NCI plot and QTAIM computational tools show the structure directing role of H-bonds combined with O \cdots CR and antiparallel π -stacking interactions in the solid state of **1**.

Acknowledgments

M.M. gratefully acknowledges financial support from Ferdowsi University of Mashhad (Grant No. 3/50674), the Iran Science Elites Federation (ISEF), Zeolite and Porous Materials Committee of Iranian Chemical Society and Iran National Science Foundation (INSF). M.M. also acknowledge the Cambridge Crystallographic Data Centre (CCDC) for access to the Cambridge Structural Database. JTM thanks Tulane University for support of the Tulane Crystallography Laboratory. We thank the MICIU/AEI from Spain for financial support (project numbers CTQ2017-85821-R and PID2020-115637GB-I00, FEDER funds).

Appendix A. Supplementary data

CCDC 2063600 and 2063337 contain the supplementary crystallographic data for **1** and **2**. These data can be obtained free of charge via <http://www.ccdc.cam.ac.uk/conts/retrieving.html>, or from the Cambridge Crystallographic Data Centre, 12 Union Road, Cambridge CB2 1EZ, UK; fax: (+44) 1223-336-033; or e-mail: deposit@ccdc.cam.ac.uk.

CRediT author statement

Mahmood Akbari, Amir Sh. Saljooghi, Nahid Lotfian, Samaneh Sadeghzadeh, Maral Aghamohammadi, Behrouz Notash and Rosa M. Gomila: Conceptualization, Methodology, Software. Masoud Mirzaei, Joel T. Mague: Data curation, Writing- Original draft preparation. Samaneh Sadeghzadeh, Maral Aghamohammadi, Behrouz Notash and Rosa M. Gomila: Visualization, Investigation. Masoud Mirzaei and Antonio Frontera: Supervision.: Masoud Mirzaei, Joel T. Mague and Antonio Frontera: Validation.: Masoud Mirzaei, Joel T. Mague and Antonio Frontera: Writing- Reviewing and Editing,

Declaration of interests

The authors declare that they have no known competing financial interests or personal relationships that could have appeared to influence the work reported in this paper.

References

- [1] M. Bazargan, M. Mirzaei, A. Franconetti, A. Frontera, Dalton Trans. **2019**, 48, 5476-5490.
- [2] S. Taleghani, M. Mirzaei, H. Eshtiagh-Hosseini, A. Frontera, Coord. Chem. Rev. **2016**, 309, 84-106.
- [3] M. Mirzaei, H. Eshtiagh-Hosseini, M. Alipour, A. Frontera, Coord. Chem. Rev. **2014**, 275, 1-18.
- [4] W. L. Leong, J. J. Vittal, Chem. Rev. **2011**, 111, 688-764.

- [5] C.L. Xiao, Q.Y. Wu, L. Mei, L.Y. Yuan, C.Z. Wang, Y.L. Zhao, Z.F. Chai, W.Q. Shi, Dalton Trans. **2014**, 43, 12470-12473.
- [6] R. Decadt, K. Van Hecke, D. Depla, K. Leus, D. Weinberger, I. Van Driessche, P. Van Der Voort, R. Van Deun, Inorg. Chem. **2012**, 51, 11623-11634.
- [7] M. Mirzaei, H. Eshtiagh-Hosseini, N. Lotfian, A. Salimi, A. Bauzá, R. Van Deun, R. Decadt, M. Barceló-Oliver, A. Frontera, Dalton Trans. **2014**, 43, 1906-1916.
- [8] M. Mirzaei, F. Sadeghi, K. Molcanov, J. K. Zareba, R. M. Gomila, A. Frontera, Cryst. Growth Des. **2020**, 20, 1738-1751.
- [9] M.A. Lashley, A.S. Ivanov, V.S. Bryantsev, S. Dai, R.D. Hancock, Inorg. Chem. **2016**, 55, 10818-10829.
- [10] D. L. Melton, D. G. VanDerveer, R. D. Hancock, Inorg. Chem. **2006**, 45, 9306-9313.
- [11] N. E. Dean, R. D. Hancock, C. L. Cahill, M. Frisch, Inorg. Chem. **2008**, 47, 2000-2010.
- [12] N. J. Williams, N. E. Dean, D. G. VanDerveer, R. C. Luckay, R. D. Hancock, Inorg. Chem. **2009**, 48, 7853-7863.
- [13] M. D. Ogden, S. I. Sinkov, M. Nilson, G. J. Lumetta, R. D. Hancock, K. L. Nash, J. Solution Chem. **2013**, 42, 211-225.
- [14] A. Moghimi, R. Alizadeh, A. Shokrollahi, H. Aghabozorg, M. Shamsipur, A. Shockravi, Inorg. Chem. **2003**, 42, 1616-1624.
- [15] L. L. Fan, C. J. Li, Z. S. Meng, M. L. Tong, Eur. J. Inorg. Chem. **2008**, 3905-3909.
- [16] M. Alipour, O. Akintola, A. Buchholz, M. Mirzaei, H. Eshtiagh-Hosseini, H. Górls, W. Plass, Eur. J. Inorg. Chem. **2016**, 5356-5365.
- [17] M. Mirzaei, A. Hassanpoor, H. Alizadeh, M. Gohari, A. J. Blake, J. Mol. Struct. **2018**, 1171, 626-630.
- [18] B. Ramezanpour, M. Mirzaei, V. Jodaian, M. Niknam Shahrak, A. Frontera, E. Molins, Inorg. Chim. Acta **2019**, 484, 264-275.

- [19] Z. Khoshkhan, M. Mirzaei, H. Eshtiagh-Hosseini, M. Izadyar, J. T. Mague, M. Korabik, *Polyhedron* **2021**, 194, 114903.
- [20] S. Derakhshanrad, M. Mirzaei, C. Streb, A. Amiri, C. Ritchie, *Inorg. Chem.* **2021**, 60, 3, 1472-1479.
- [21] M. Bazargan, M. Mirzaei, A. Amiri, C. Ritchie, *Microchim. Acta*, **2021**, 188, 108.
- [22] R.F.W. Bader, *Chem Rev.* **1991**, 91, 893–928
- [23] E. R. Johnson, S. Keinan, P. Mori-Sanchez, J. Contreras-Garcia, A. J. Cohen, and W. Yang, *J. Am. Chem. Soc.* **2010**, 132, 6498
- [24] C.J. Chandler, L.W. Deady, J.A. Reiss, *J. Heterocyclic Chem.* **1981**, 18, 599-601.
- [25] Stoe & Cie, X–AREA: Program for the Acquisition and Analysis of Data, Version 1.30; Stoe & Cie GmbH: Darmstadt, Germany, 2005.
- [26] L. J. Farrugia, *J. Appl. Cryst.* **1999**, 32, 837-838.
- [27] D.T. Cromer, J.T. Waber, *International Tables for X-ray Crystallography*, the kynoch Press, Birmingham, England, **1974**.
- [28] Stoe and Cie, X-STEP32. Version 1.07e; Stoe and Cie: Darmstadt, Germany, **2000**.
- [29] G.M. Sheldrick, *Acta Cryst. A* **2008**, 64, 112-122.
- [30] SADABS 2.10 and SAINT, Bruker-AXS inc. **2002**, Madison, WI, U.S.A.
- [31] L. J. Farrugia, *J. Appl. Cryst.* **1997**, 30, 565-565.
- [32] L. J. Farrugia, *J. Appl. Cryst.* **1999**, 32, 837-838.
- [33] G. M. Sheldrick, *Acta Cryst. C* **2015**, 71, 3-8.
- [34] A.D. Becke, *Phys. Rev. A* **1988**, 38, 3098– 3100.
- [35] J. P. Perdew, *Phys. Rev. B* **1986**, 33, 8822– 8824.
- [36] F. Weigend, *Phys. Chem. Chem. Phys.* **2006**, 8, 1057.

- [37] S. Grimme, J. Antony, S. Ehrlich, H. Krieg, *J. Chem. Phys.* **2010**, 132, 154104.
- [38] R. Ahlrichs, M. Bär, M. Hacer, H. Horn, C. Kömel, *Chem. Phys. Lett.* **1989**, 162, 165.
- [39] S.F. Boys, F. Bernardi, *Mol. Phys.* **1970**, 19, 553
- [40] J. Contreras-Garcia, E.R. Johnson, S. Keinan, R. Chaudret, J.P. Piquemal, D.N. Beratan, W. Yang, *J. Chem. Theory Comput.* **2011**, 7, 625.
- [41] T. Lu and F. Chen, *J. Comput. Chem.* **2012**, 33, 580–592.
- [42] J W. Humphrey, A. Dalke and K. Schulten, *J. Mol. Graph.* **1996**, 14, 33–38.
- [43] E. Espinosa, E. Molins, C. Lecomte, *Chem. Phys. Lett.*, **1998**, 285, 170

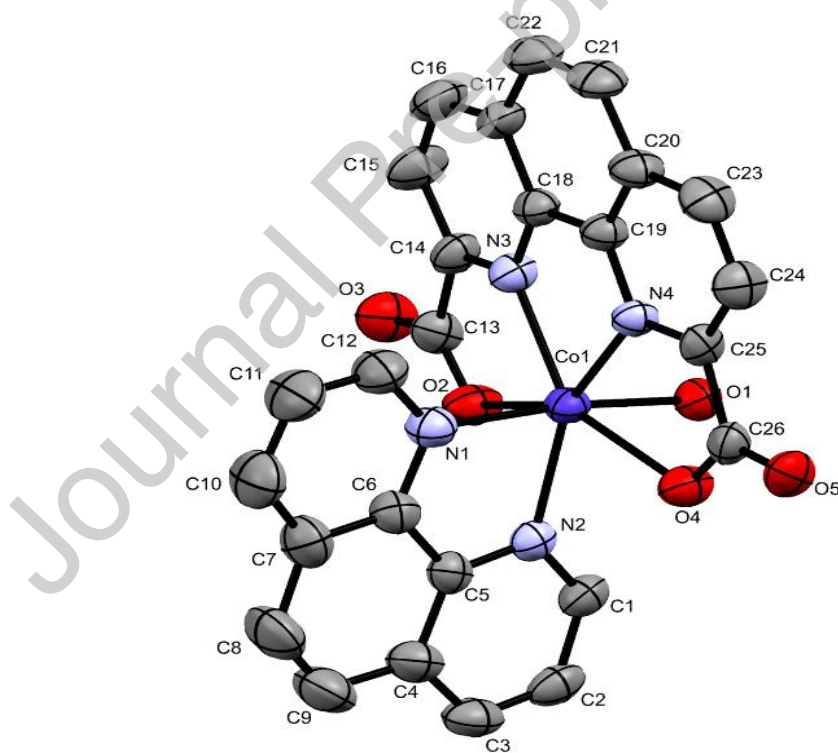


Figure 1. ORTEP drawing of the **1** with thermal ellipsoids shown at the 50% probability level. The uncoordinated solvent molecules and H atoms are omitted for clarity.

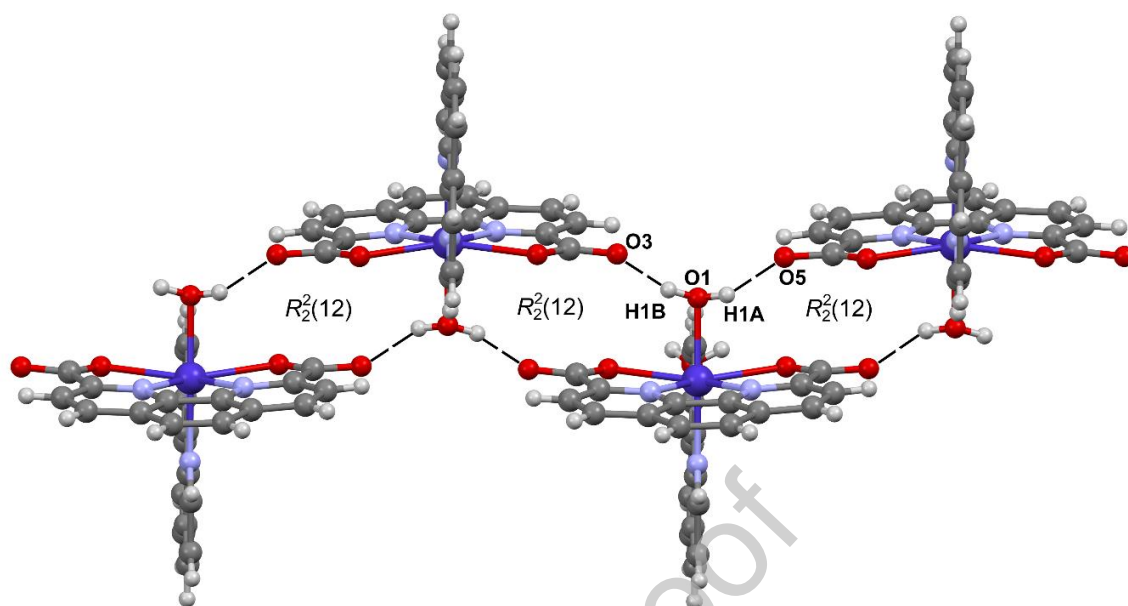


Figure 2. Part of the crystal structure of **1** showing the formation of one O-H...O hydrogen-bonded zigzag chain with a (a) $R_2^2(12)$ graph set.

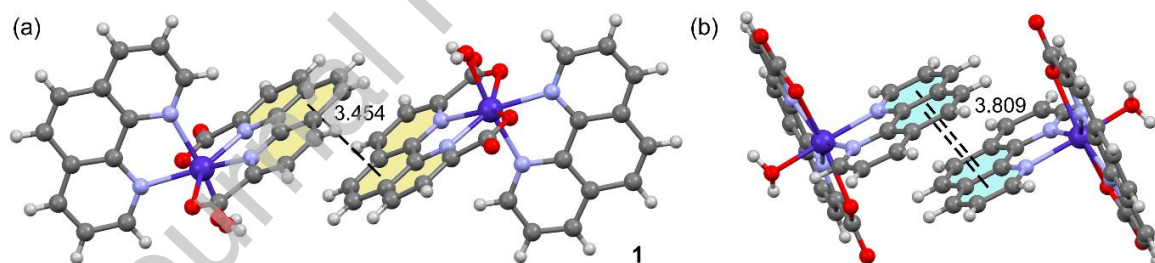


Figure 3. Representation of two self-assembled dimers formed by $\pi\cdots\pi$ interactions involving PDA (a) and *phen* (b) ligands in **1**.

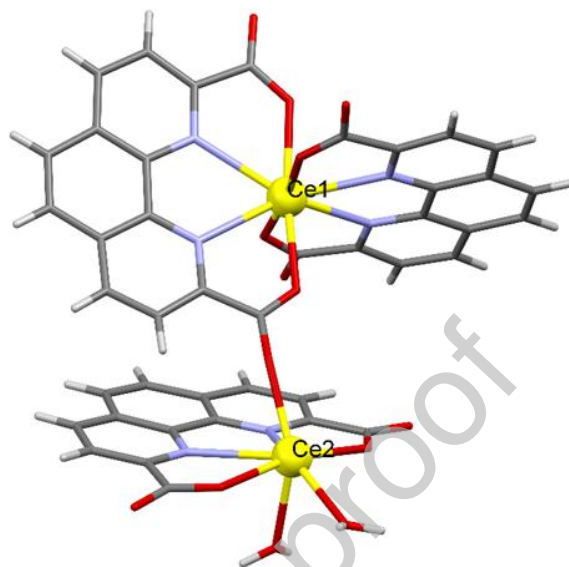


Figure 4. Asymmetric unit of 2. Uncoordinated water molecules are omitted for clarity.

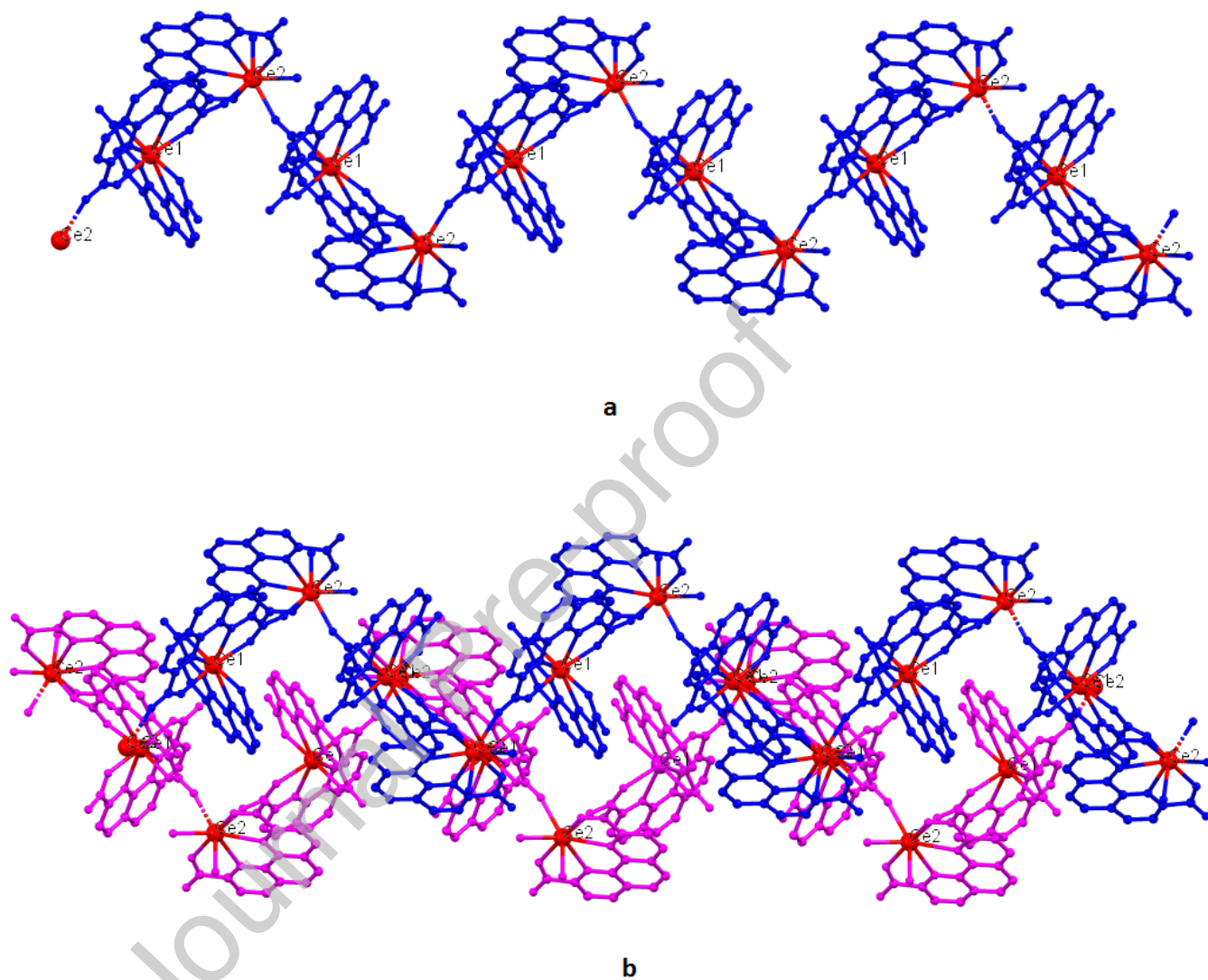


Figure 5. (a) The single helix chain (b) and the alternately packed right-handed and left-handed helices in **2**. The helical axis is parallel to the *b* axis.

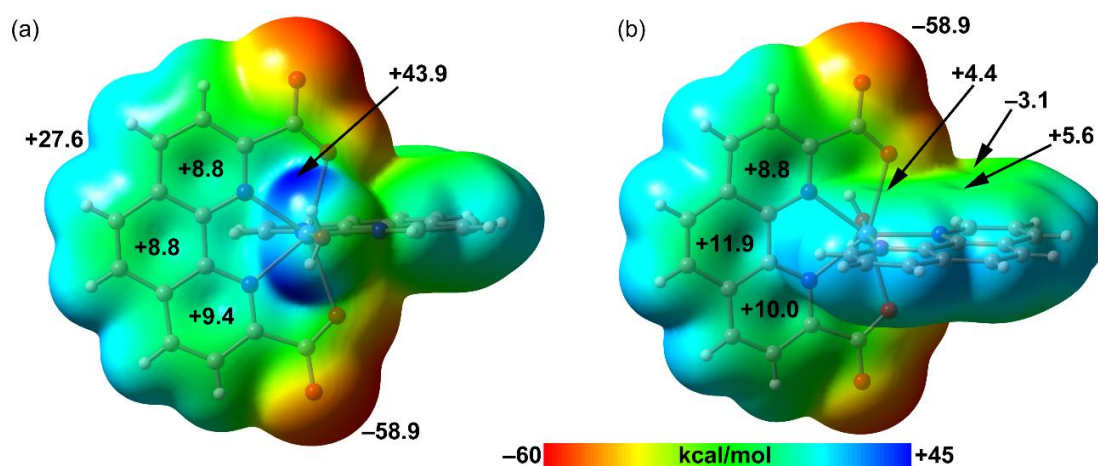


Figure 6. Two opposite views, “water up” (a) and “water down” (b), of the MEP surface of **1** at the RI-BP86-D3/def2-TZVP level of theory (isosurface 0.001 a.u.).

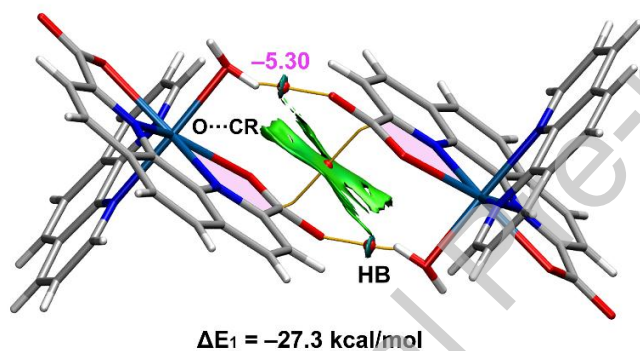


Figure 7 QTAIM (bond CPs in red) and NCI index analyses of the $R_2^2(12)$ synthon of **1**. The gradient cut-off is $\rho = 0.04$ a.u., isosurface $s = 0.5$, and the colour scale is -0.04 a.u. $\langle \text{sign}\lambda_2 \rangle \rho < 0.04$ a.u. Only intermolecular interactions are shown. The strength of the H-bond is indicated in fuchsia next to the bond CPs.

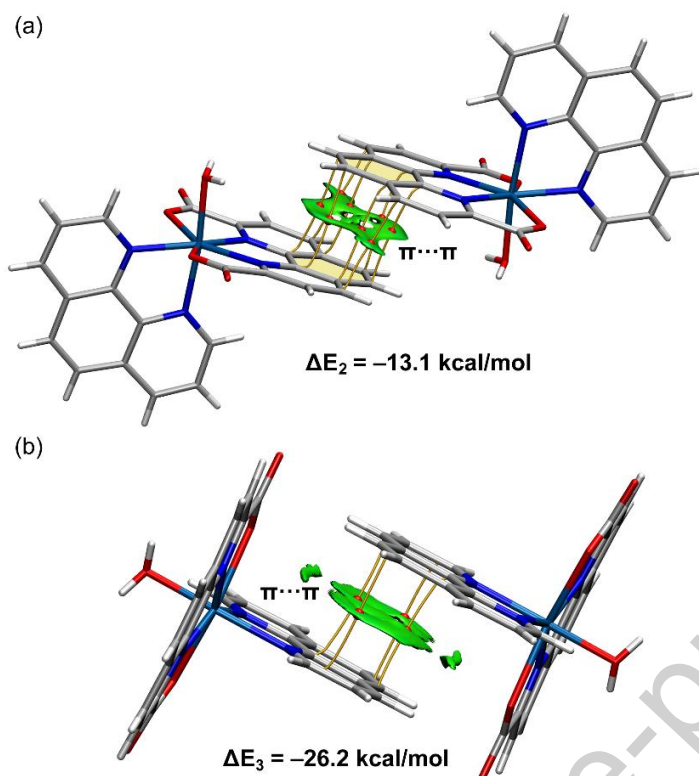


Figure 8. QTAIM (bond CPs in red) and NCI index analyses of the antiparallel PDA...PDA (a) and *phen*...*phen* (b) π -stacking assemblies of **1**. The gradient cut-off is $\rho = 0.04 \text{ a.u.}$, isosurface $s = 0.5$, and the colour scale is $-0.04 \text{ a.u.} < (\text{sign}\lambda_2)\rho < 0.04 \text{ a.u.}$ Only intermolecular interactions are shown.

Table 1. X-ray diffraction crystallographic data and structure refinements for **1** and **2**

	1	2
Empirical formula	C ₂₈ H ₂₁ CoN ₅ O ₆	C ₄₂ H ₂₈ Ce ₂ N ₆ O ₁₇
Formula weight	582.43	1168.95
Temperature (K)	298(2)	150(2)
Crystal system	Triclinic	Monoclinic
Space group	<i>P</i> $\bar{1}$	<i>P</i> 2 ₁ / <i>c</i>
<i>a</i> (Å)	10.478(2)	14.2234(8)
<i>b</i> (Å)	10.581(2)	18.5431(10)
<i>c</i> (Å)	12.237(2)	15.7009(8)
α (°)	90.65(3)	90
β (°)	106.64(3)	103.690(2)
γ (°)	103.09(3)	90
<i>V</i> (Å ³)	1261.9(5)	4023.4(4)
<i>Z</i>	2	4
<i>D</i> _{calc} (g cm ⁻³)	1.533	1.930
μ (mm ⁻¹)	0.735	2.323
<i>F</i> (000)	598	2296
Reflections collected	9341	15410
<i>R</i> ₁ ^a , <i>wR</i> ₂ ^b [<i>I</i> > 2 σ (<i>I</i>)]	0.0613, 0.1309	0.0217, 0.0498
GOF	0.9	1.045
CCDC	2063600	2063337

^a $R_1 = \sum ||F_o| - |F_c|| / \sum |F_o|$. ^b $wR_2 = \{ \sum w(F_o^2 - F_c^2)^2 / \sum w(F_o^2)^2 \}^{1/2}$.